Cross validation of analytical solutions against the computational model predictions of the response of end bearing energy pile

Arash Saeidi Rashk Olia[1], and *Dunja* Perić[1,*]

[1]Kansas State University, Department of Civil Engineering, 1701C Platt St., Manhattan, KS 66506-5000, US

Abstract. Predictions of responses of a single energy pile to a combined mechanical and thermal loading are presented. They were obtained from computational and analytical models. The former model provided predictions based on a coupled thermal hydro-mechanical finite element analysis while the predictions of the latter were obtained from the recently derived analytical solutions. The energy pile is surrounded by a single uniform soil layer underlain by a very stiff bedrock. Two scenarios of temperature history were considered. In the first scenario the pile remained in a net heated state while the second one induced a net cooled state. In both loading scenarios a compressive axial load was applied at the pile head prior to the thermal loading. The net heating induced an upward axial displacement, tensile strain and compressive stress while the net cooling induced a downward vertical pile displacement, compressive strain and tensile stress. In spite of different methods of obtaining the soil stiffness for computational and analytical models the predictions of the axial pile displacement, stress and strain show a very good agreement.

1 Introduction

Thermo-active geo-structural elements such as energy piles transfer thermal energy and load between the superstructure and the subsurface. The former is accomplished by embedding plastic pipes into energy pile, thus enabling the transfer of thermal energy. Temperature in the ground at depths between 3 and 5 m is constant and approximately equal to the mean annual air temperature [1]. This allows the ground storage of the excess heat in summer, and its subsequent extraction of in winter, thus providing a supplemental space heating.

The free thermal deformation of energy piles is restrained by the surrounding soil, thus leading to thermally induced displacement, strain and stress in the piles. Consequently, design of energy piles requires understanding of the thermo-mechanical soil structure interaction and thermally induced stresses. To this end, various researchers have developed physical and numerical models of energy piles. The former primarily encompass full-scale in situ tests and geotechnical centrifuge tests, while the latter mostly rely on finite element and finite difference modeling.

The current study presents a cross validation between two different mathematical methods including analytical modeling and Finite Element Analysis (FEA). Specifically, predictions of axial displacement, strain and stress obtained by using these two methods are presented and compared.

2 Analytical model

Cossel 2019 [2] and Perić et al. 2020 [3] derived analytical solutions for thermo-mechanical soil structure interaction in energy piles, thus providing expressions for axial displacement, strain and stress. The pile was subjected to a combined thermal and mechanical load. The former comprised heating or cooling of the energy pile while the latter included an axial load applied at the pile head. They assumed that both, the pile and the soil pile interface remained in elastic regime under working stresses. These assumptions were confirmed by several other researchers [3-7], thus enabling the use of a continuous linear elastic shear spring that characterizes the soil pile interface. Furthermore, the pile was assumed to obey a thermo-elastic constitutive law. In the case of end bearing piles, the axial displacement at the pile tip was assumed to be zero in the analytical model, in order to simulate the ideal hard bedrock effect. Head of the pile in the current study is free to move under both, thermal and mechanical loading, as no restriction has been applied at the pile head.

* Corresponding author: peric@ksu.edu

3 Material properties

In order to cross validate the numerical model against analytical solutions a semi-hypothetical homogeneous soil profile was developed. For this purpose, one of the four soil layers surrounding the energy pile constructed and tested at Swiss Federal Institute of Technology Lausanne, Switzerland (Laloui et al. [4]) was chosen. Based on laboratory classification tests, the results of which were provided by Laloui et al. [8], and in accordance with the Unified Soil Classification System each of the four soil layers at the site classifies as a low plasticity clay (CL). These layers are underlain by the sandstone whose top surface is located at a depth of 25.5 meters. Specifically, the top two layers (A1 and A2) are alluvial glacial lacustrine deposits. In the present study, a single soil layer, representing the soil A1 from Laloui et al [4] is placed on top of the bedrock, which coincides with the pile tip elevation.

Elastic parameters of soil A1 used herein were independently calibrated by Perić et al. [5] according to the site investigation report provided by Laloui et al. [8]. Therefore, the effective elastic modulus of soil A1 is 190 MPa and its effective Poisson's ratio is 0.22. The remaining soil properties used in the computational model, except for the elastic moduli of the bedrock, were taken from Laloui et al. [4]. Therefore, for soil A1 the coefficients of thermal expansion, heat capacity and thermal conductivity are equal to 1×10^{-5} /°C, 2.4×10^{6} J/(m^3°C) and 1.8 W/(m°C) respectively, while for the bedrock the coefficients of thermal expansion, heat capacity and thermal conductivity are equal to 1×10^{-6}/°C, 2.0×10^{6} J/(m^3°C) and 1.1 W/(m°C) respectively.

It is because the analytical model enforces zero axial displacement at the pile tip that the effective elastic modulus of the bedrock used herein is much larger than the one reported by Laloui et al. [4]. Specifically, the value of the effective Young's modulus of 50.5 GPa and of the effective Poisson's ratio of 0.18 selected herein correspond to the realistic possible maximum values for rock [9]. Additionally, the hydraulic conductivities of soil A1 and the bedrock are equal to 2×10^{-6} m/s and 1×10^{-15} m/s respectively. The shear spring stiffness substituting soil A1 in the analytical model was equal to 16.7 MPa/m, thus corresponding to the value reported by Knellwolf et al. [7].

The thermal expansion, heat capacity and thermal conductivity of the pile are equal to 1×10^{-5} /°C, 2×10^{6} J/(m^3°C), and 2.1 W/(m°C) respectively. Finally, the elastic modulus and the Poisson's ratio of the pile are equal to 29.2 GPa and 0.177 respectively.

4 Mechanical and thermal loads

A compressive axial load having a magnitude of 1000 kN was applied at the pile head. In addition, the pile was subjected to two different thermal loading scenarios of net heating and net cooling. The former consisted of a single heating/cooling cycle while the latter included a single cooling/heating cycle. Table 1 presents the corresponding temperature histories whereby the positive temperature difference (ΔT) indicates heating of the energy pile with respect to the surrounding soil. In the first scenario the pile remains in a net heated state while in the second one it stays in a net cooled state with respect to its initial temperature. It should be noted that the negative temperature difference does not necessarily indicate that the soil in freezing, because it represents the difference between the pile and the soil temperatures.

Table 1. Temperature histories for two loading scenarios

Time (days)	0	5	22	27	62
ΔT (°C)	0	9	14	6	2
ΔT (°C)	0	-9	-14	-6	-2

5 Computational model

A coupled thermal hydro-mechanical FEA was performed by using the finite element software ABAQUS/CAE 2019. The pile diameter is equal to 1 m while its length is 26 m in accordance with the dimensions reported by Laloui et al. [4].

Figure 1 depicts the colour map of temperatures corresponding to ΔT = 14°C superimposed on the deformed finite element mesh, thus showing the computational model. Horizontal displacements are prevented along the vertical boundaries, while the full fixity is enforced along the bottom boundary.

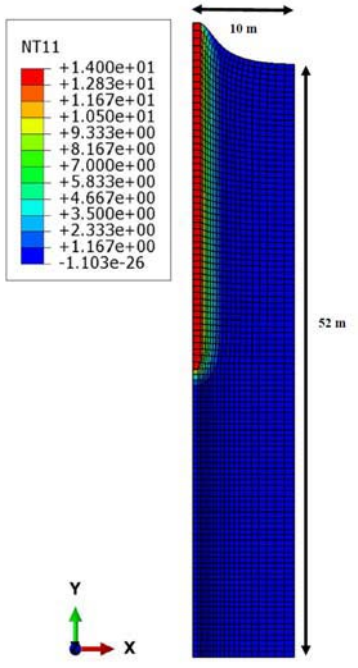

Fig. 1. Temperature distribution (in °C) corresponding to ΔT=14°C predicted by the computational model (deformation scale factor = 2200)

The fully coupled pore pressure displacement analyses were conducted by using the eight-node biquadratic axisymmetric quadrilateral elements with reduced integration (CAX8RP) for the soil and bedrock,

and the biquadratic axisymmetric quadrilateral elements with reduced integration (CAX8R) for the pile. Heat transfer analysis was performed by using the eight-node quadratic axisymmetric heat transfer quadrilateral elements (DCAX8).

The analysis was performed in two steps. The first step comprised solely the thermal analysis while the second one included the coupled pore pressure displacement analysis. Specifically, the first step provided the temperature distribution within the domain, which was subsequently used as input into the second step, within which the axial compressive load of 1000 kN was applied at the pile head. A rough contact between the pile and soil was used in accordance with the assumption of elastic states of the soil and the pile. In both, analytical and numerical models, a uniform temperature along the energy pile was enforced.

6 Cross validation

Compressive strain and stress are negative while the upward displacement is positive. Figure 2 shows a vertical head displacement of the energy pile versus time. The initial head displacement is negative due to the axial compressive load for both, net heating and net cooling. As expected, the extreme values of the vertical head displacement occur at $\Delta T = \pm$ 14°C. Furthermore, the pile expands during the net heating scenario, and contracts during the net cooling scenario. Thus, the magnitude of axial displacement is smaller in the case of net heating than in the case of net cooling. In the case of net heating the initial downward displacement induced by the axial compressive load is compensated by the upward heating induced displacement at around 3°C to 4°C.

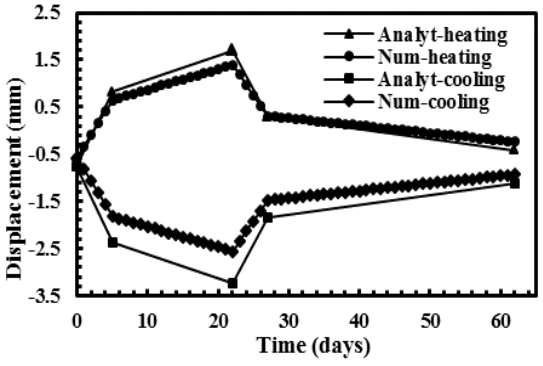

Fig. 2. Vertical pile head displacement versus time for net heating and net cooling

Figures 3 and 4 show the axial displacement of the pile versus depth at five and 22 days after the beginning of the net heating and the net cooling respectively. As expected, the numerically predicted displacement of the pile tip is negligible, thus agreeing very well with the assumption used by analytical solutions.

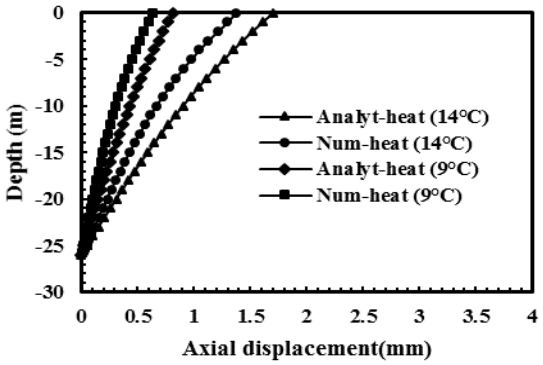

Fig. 3. Axial displacement in the pile versus depth at ΔT = 9°C and 14°C

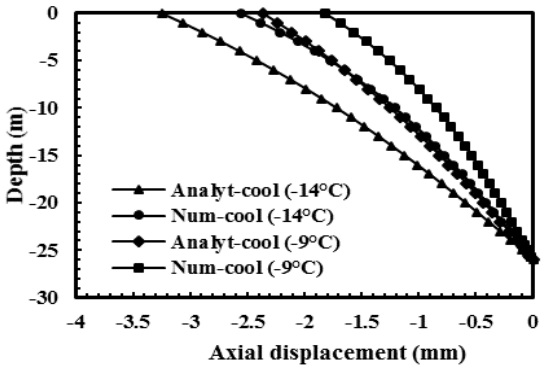

Fig. 4. Axial displacement in the pile versus depth at ΔT = -9°C and -14°C

Furthermore, the extreme values of displacements occur at the pile head. Predictions of analytical and computational models follow the same trend of change versus depth and show a reasonable agreement while exhibiting a small discrepancy between the predicted values. The discrepancy slightly increases with the increasing temperature change. It is because the pile tip is practically fixed in both models that the discrepancy is primarily caused by the discrepancy between the soil stiffness values used in the analytical and computational models. Specifically, the elastic stiffness of the shear spring was determined from the in-situ pile test, while the elastic stiffness moduli of the soil were determined from the conventional triaxial test. Thus, the soil stiffness used by the two modeling approaches are not effectively equal to each other. Moreover, it is noted that the increase in discrepancy between numerical and analytical predictions with the increasing temperature is due to the resulting increase in the pile displacement, not due to the increased temperature difference itself. This is the reason for occurrence of the larger discrepancy in the case of net cooling. In this case, the pile contraction due to cooling is added to the pile contraction induced by the mechanical load. On the contrary, during the net heating the initial contraction is subtracted from thermally induced expansion, thus resulting in the smaller net displacement than in the case of net cooling, the temperature differences of 9°C and 14°C are larger than the temperature differences of 3°C to 4°C that are

required for a full compensation of head displacement between heating and mechanical load. Thus, the overall behavior is in this case governed by heating and similarly by cooling as opposed to the mechanical load. Furthermore, the axial displacement of the pile is positive in net heating scenario as shown in Figure 3.

Figures 5 and 6 depict the numerical and analytical predictions for the axial strain of the pile versus depth at five and 22 days after the beginning of the net heating and the net cooling respectively. Again, the predictions of the numerical and analytical models are closer to each other at the smaller temperature difference, which is a consequence of the lower displacements that occur at lower temperatures. Furthermore, the difference between the strains predicted by numerical and analytical models is larger in the case of cooling due to the larger magnitude of the corresponding displacements. The differences decrease in the vicinity of the pile tip due to the large stiffness of the bedrock used in the numerical model.

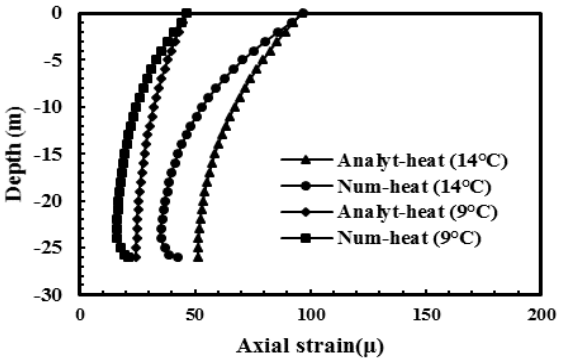

Fig. 5. Axial strain in the pile versus depth at ΔT= 9°C and 14°C

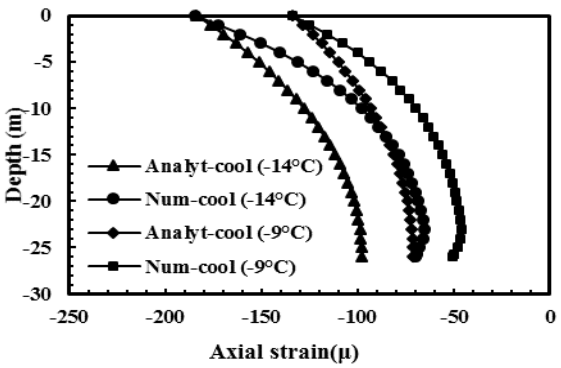

Fig. 6. Axial strain in the pile versus depth at ΔT = -9°C and -14°C

The numerical and analytical predictions of the axial or vertical stress in the pile versus depth at five and 22 days after the beginning of the net heating and the net cooling are shown in Figures 7 and 8 respectively. Although the amount of discrepancy between the axial stress predictions slightly increases with the increased temperature change the overall difference versus depth remains reasonable. The mechanical stresses predicted by computational and analytical models show a very good agreement. The combination of compressive force and heating results in an increased compressive stress in the pile as compared to the mechanically induced stress, as shown in Figure 7.

Figure 8 shows that the energy pile in the case of net cooling scenario is prone to development of a tensile stress zone. Axial stress in the pile induced by a compressive axial load is always negative. Nevertheless, the net cooling induces tensile stress. Thus, the tensile zone that results from a combined mechanical load and cooling extends upward from the pile tip and it is larger in the case of a larger temperature decrease.

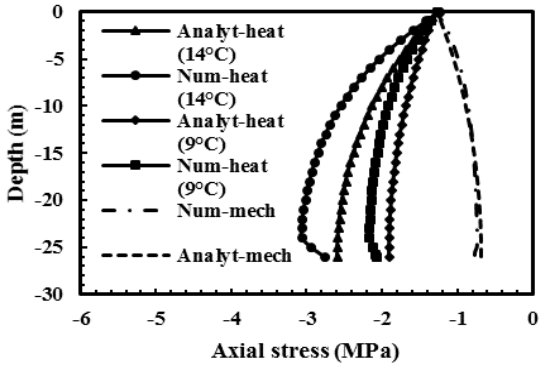

Fig. 7. Axial stress in the pile versus depth at ΔT = 9°C and 14°C

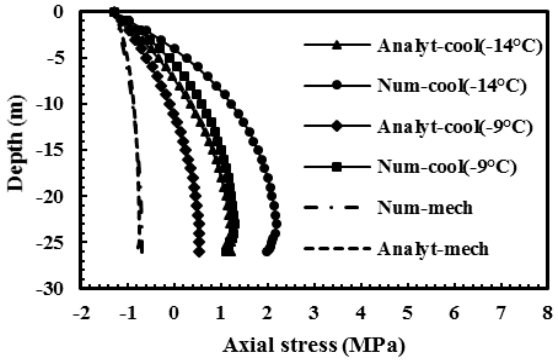

Fig. 8. Axial stress in the pile versus depth at ΔT = -9°C and -14°C

7 Conclusions

Numerical and analytical predictions for the vertical displacement, strain and stress in a single end bearing energy pile subjected to a combined mechanical and thermal load have been successfully cross validated. The difference between the predictions remained reasonable up to ± ΔT =14°C and it mainly depends on the difference between the soil stiffness employed by the two models. Moreover, the discrepancy between the predictions of the two models increases with increase in the temperature difference, thus resulting in larger magnitude of displacements.

For the selected magnitude of thermal and mechanical loads the predictions demonstrate that the net heating causes upward displacement, tensile strain and compressive stress while the net cooling induces downward displacement, compressive strain and tensile stress in the energy pile. Additionally, the results show that the head displacement induced by mechanical compressive load was fully compensated by the net heating in the amount of ΔT = 3°C to 4°C. This implies that the behaviour of the energy pile beyond this temperature is mostly governed by heating. The net cooling scenario results in the development of a tensile stress zone in the pile, which extends upwards from the pile tip. The exact length of the tensile zone depends on the amount of cooling whereby a larger tensile zone develops in the case of a larger magnitude of cooling. Furthermore, the analytical model predicts development of the maximum tensile stress at the pile tip, while the computational model predicts development of maximum tensile stress slightly above the pile tip.

References

1. A. Burger, E. Recordon, D. Bovet, L. Cotton, & B. Saugy, "*Thermique des Nappes Souterraines*" Presses Polytechniques Romandes. Laussane, Switzerland (1985).
2. A. Cossel, *Analytical solutions for thermo-mechanical soil structure interaction in energy piles,* Kansas State University, MS thesis (2019).
3. D. Perić, A. Cossel, & E. Sarna, S. A. "*Analytical Solutions for Thermomechanical Soil Structure Interaction in End-Bearing Energy Piles*". Journal of Geotechnical and Geoenvironmental Engineering, **146**(7), 04020047, (2020). https://doi.org/10.1061/(ASCE)GT.1943-5606.0002269.
4. L. Laloui, M. Nuth, & L. Vulliet. "*Experimental and numerical investigations of the behaviour of a heat exchanger pile"* International Journal for Numerical and Analytical Methods in Geomechanics, **30**(8), 763-781, (2006). https://doi.org/10.1002/nag.499.
5. D. Perić, T. V. Tran, M. Miletić, "*Effects of soil anisotropy on a soil structure interaction in a heat exchanger pile*" Computers and Geotechnics, **86**, 193-202, (2017). https://doi.org/10.1016/j.compgeo.2017.01.005.
6. C. Iodice, R. Di Laora, & A. Mandolini, "*Analytical Solutions for Ultimate Limit State Design of Thermal Piles,* " Journal of Geotechnical and Geoenvironmental Eng., **146**(5), 04020016, (2020). https://doi.org/10.1061/(ASCE)GT.1943-5606.0002204.
7. C. Knellwolf, H. Peron, & L. Laloui, *"Geotechnical analysis of heat exchanger piles"* Journal of Geotechnical and Geoenvironmental Engineering, **137**(10), 890-902, (2011). https://doi.org/10.1061/(ASCE)GT.1943-5606.0000513.
8. L. Laloui, M. Moreni, G. Steinmann, L. Vulliet, A. Fromentin, D. Pahud, "*Heat exchanger pile: effect of the thermal solicitations on its mechanical properties"* Report of the Swiss Federal Office of Energy, (1999).
9. A. Palmström & R. Singh, *"The deformation modulus of rock masses—comparisons between in situ tests and indirect estimates"* Tunnelling and Underground Space Technology, **16**(2), 115-131, (2001). https://doi.org/10.1016/S0886-7798(01)00038-4.